Circumstellar C2 Absorption Lines in Carbon Stars

presented by: Hideyuki Izumiura (OAO, NAOJ)

collaborators: Rie Kimata & Ryukoh Hirata (Kyoto-U.)

1) Detections of circumstellar C_2 absorption lines in optical carbon stars, including $^{12}C^{13}C$ and $^{13}C^{13}C$ lines, are presented.

2) Observed porperties of the circumstellar C_2 gas, such as the rotational excitation temperature and column density, are derived.

3) Possible origin of the circumstellar C_2 gas is discussed.

1. Introduction

¥ Study of mass-loss from AGB stars

	Optical	Infrared	Radio
O-rich:	Atm/---	---/Mol	Atm/Mol
C-rich:	-----/---	---/Mol	Atm/Mol

We intended to detect a signature of mass-loss in molecular lines in the optical region using HIDES in C-rich stars.

¥ Presence of circumstellar C_2 absorption lines in mass-losing AGB and post-AGB stars:

***Bakker et al. (1996, 1997)**
-- Detection of circumstellar C_2 lines in a dozen carbon-rich post-AGB stars, which were interpreted to be formed in their AGB remnant shells.

-- Circumstellar C_2 absorption lines were also detected in IRC+10216, the only example ever known among currently mass-losing AGB stars.

***Izumiura et al. (2002)**
-- Clear detection of circumstellar C_2 and the isotopomers' Swan (0,0) band absorption lines in several bright optical carbon stars.

↓

¥ Circumstellar C_2 could be a new probe of the circumstellar envelopes of optical carbon stars ⇒ Ve, Trot, N(C_2), $^{12}C/^{13}C$

We thus performed high resolution spectroscopic observations of 44 carbon stars.

2. Observation

***Observation dates:**
1999/12/27- 31, 2000/01/03,18, 02/22-24, 12/22, 2001/02/13-17, 2001/04/02-07, 07/30, 08/13-15, 08/24-29 (total : 32 nights)
*** Instrument: HIDES (HIgh Dispersion Echelle Spectrograph)**
*** Spectral resolution: ~ 95,000 (3km/s)**
*** Coverage: ~ 1100Å centered at Swan(0,0) bandhead(~5165Å)**
*** Sample: 44 bright optical carbon stars (⇒ Table.1) from Lambert et al. (1986,ApJS,62,373) + additional stars**

Table.1 List of sample stars

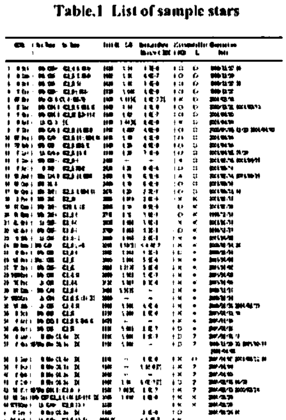

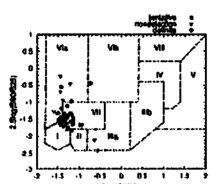

Fig.1 IRAS two-colour diagram of the sample

3. Results

3.1 Detection/nondetection of circumstellar C_2 absorption lines

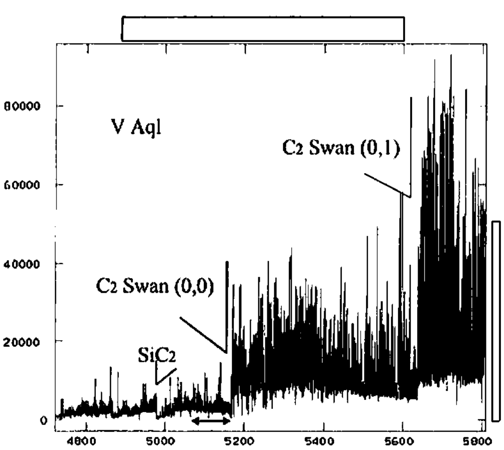

Fig.2 Green spectrum of a N-type carbon star, V Aql. Red arrow indicates the region analysed in this study

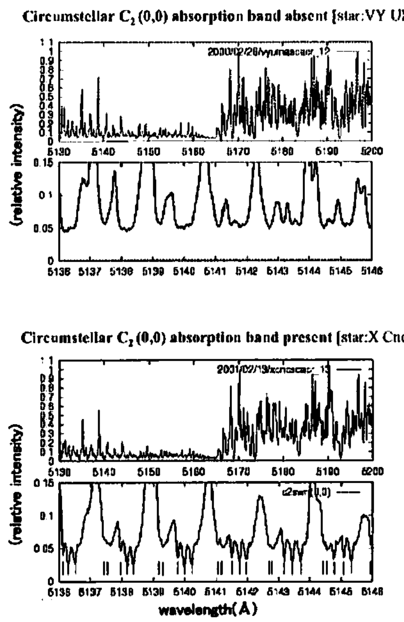

Fig.3 Examples of the spectra with and without circumstellar C_2 lines.

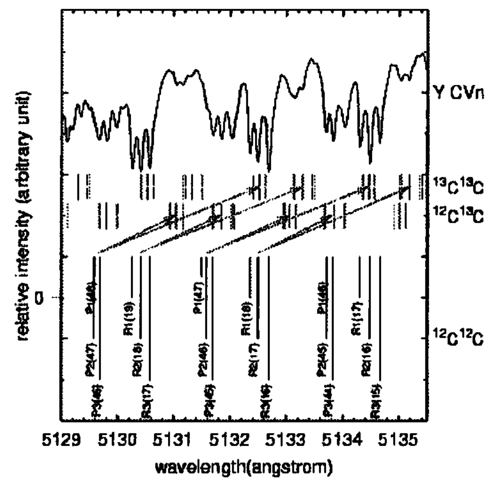

Fig.4 Isotopomers' ($^{13}C^{12}C$ and $^{13}C^{13}C$) lines in a ^{13}C-rich (J-type) carbon star, Y CVn.

Table.2 Summary of the survey results [total : 44 stars]

	Number of stars
definite detection	17
tentative detection	6
nondetection	21

3.2 Radial velocity variation of circumstellar C_2 absorption lines

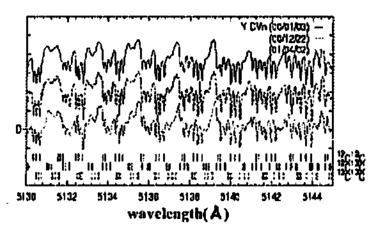

Fig.5 Three spectra at different dates separated by more than a year of Y CVn

Table 3 Radial velocity of circumstellar C_2 gas at different epochs

Star	dates(yy/mm/dd)	$V_{C2,helio}$[km s^{-1}]
X Cnc	00/12/22	-17.43
	01/02/13	-17.38
T Cnc	01/02/16	-4.73
	01/04/07	-4.97
RY Dra	00/01/18	-13.99
	01/04/04	-13.59
Y CVn	00/01/03	14.13
	00/12/22	14.35
	01/04/02	14.25

Radial velocities of C_2 gas layer are found to be very stable on the order of 0.5 km/s

3.3. Correlation between C_2 detection and both photospheric effective temperature(Teff) and C/O abundance ratio

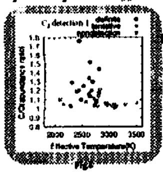

circumstellar C_2 is detected in stars with:

- Teff < 2800K
- C/O > 1.1

the formation of C_2 gas layer is sensitive to the photospheric effective temperature and chemical composition.

3.4 Comparison with circumstellar CO

Fig.7 : comparison of the expansion velocity of circumstellar C_2 with that of CO

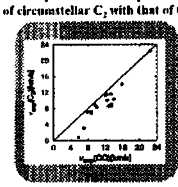

Fig.8 : correlation between C_2 detection and $\dot{M}$(CO)

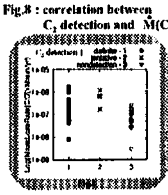

$V(C_2) < V(CO)$

⇒ $V(CO)-V(C2) = \sim 1-4$ km/s

(accuracy of the C_2 velocity is about 0.1km/s)

Circumstellar C_2 lines tend to be detected in stars with relatively higher mass loss rate derived From circumstellar CO lines, but their correlation is weak.

C_2 absorption lines are possibly formed in a different part of CSEs from that for CO lines.

according to the dust-driven wind theory, the expansion velocity increases monotonously with radius

⇒ **C_2 line-forming region could locate at the innermost part of the CSEs of the carbon stars, just inside the place where the outflow reaches the terminal velocity.**

3.5 Rotational excitation temperature and column density

*** We have equivalent widths of a number of rotational transition lines (about 50~150)**

then

with the assumptions below:

- **the lines are optically thin i.e., equivalent width ∝ column density**
- **Boltzmann distribution for the rotational ladder**

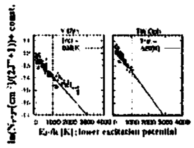

Fig.9 Rotational diagram for C_2. $N_{v''J''}$[cm^{-2}] is C_2 column density in the energy level (v'',J'')

*** Rotational excitation temperature:**

Trot = 350 ~ 800 [K] (Fig.10)

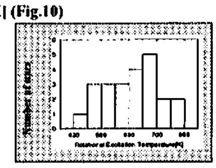

Fig.10 Rotational excitation temperature from the rotation diagram

*** Total column density assuming LTE at Trot**

$N_{C2,tot}$ = (2.29 ~ 8.62) × 10^{14}[cm^{-2}] (Fig.11)

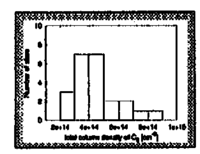

Fig.11 Total column density of C_2

3.6 Distance of the circumstellar C_2 gas layer from the star

Assumptions:

1. *Trot ≒ Tgas (kinetic temperature)*
2. *Tgas ∝ $r^{-\alpha}$*

$$\Rightarrow T_{gas}(r) = T_{gas}(r_0)\left(\frac{r_0}{r}\right)^{\alpha} \cong T_{rot}(r)$$

3. *Tgas (R_*) = Teff, R_* = r_0*

$$\Rightarrow R_{C_2} = R_*\left(\frac{T_{eff}}{T_{rot}}\right)^{\frac{1}{\alpha}}.$$

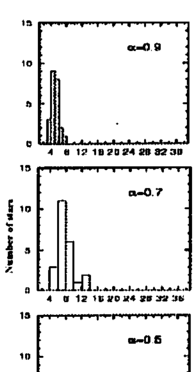

Fig. 12 Distribution of the distance of the line-forming region from the central star. Three cases of α = 0.5, 0.7, and 0.9 are indicated. According to model calculations of circumstellar envelopes, α takes values between 0.5 and 1.0 (Doty & Leung 1997, Schoier & Olofsson 2001). With the above assumptions, the line-forming regions are inferred to locate within a few tens of stellar radius.

3.7 C_2 fractional abundance and the line forming region

Based on the inferred location of the line-forming region, it is now possible to estimate the C_2 fractional abundance relative to H_2 in the line-forming region.

- **Number density of C2 molecules:**
  $n_{C2} \doteqdot N_{C2,tot} / R_{C2}$ [cm^{-3}]
  (this assumption could give rise to a significant underestimate)

- **Number density of H_2 molecules at $r=R_{C_2}$:**
  $dM/dt = 4\pi r^2 \rho v_e$
  $r = R_{C2}$, $v_e = V_{exp}(C_2)$, $\rho(R_{C2}) \doteqdot n_{H2}(R_{C2})\, m_{H2}$
  $n_{H2}(R_{C2}) \doteqdot (dM/dt)/(4\pi R_{C2}^2 V_{exp}(C_2) m_{H2})$ [cm^{-3}]

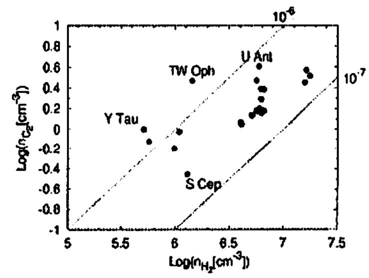

Fig. 13 Number density of C_2 versus that of H_2.

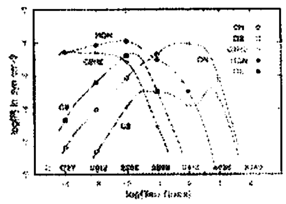

Fig. 3. The partial pressure of HCN in the model atmosphere underlying the spectra in Figs 2, 5 and 6 and lower panel of Fig. 1. The weak HCN lines are formed at $\tau \approx 10^{-1}$. Also shown is the partial pressure of other molecules (C_2, CN, C_2H_2 and C_3) that contribute to the molecular opacity. The tickmarks along the curves show decades in optical depths from $\tau \approx 10^{-4}$ (left) and upward

Jorgensen 1990

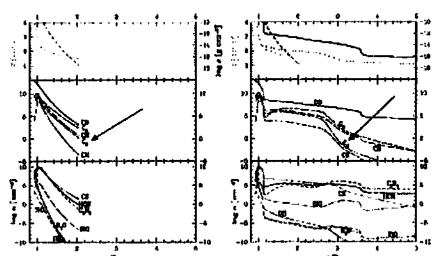

Helling and Winters 2001

¥ Model calculations:
eg. Jorgensen 1990,
Jorgensen et al. 1992,
Helling and Winters 2001

dust formation included
molecular dissociative equilibrium included

=> $n[C_2] / n[H_2] << 10^{-6}$ ouside the dust formation region

$\sim 10^{-8} < n[C_2H_2] / n[H_2] < \sim 10^{-6}$

¥ Our results:
$10^{-7} < n[C_2] / n[H_2] < 10^{-6}$ (note: uncertainty is large)

=> The observed circumstellar C_2 gas

Product of the photodissociation of C_2H_2 molecules !?

Summary:

- Circumstellar C_2 Swan (0,0) absorption lines: 44 carbon stars => 17 definite, 6 possible, 21 negative.
- Conditions for the presence: 2300 K < Te < 2800 K, C/O > 1.1.
- Vrad determination: standard error ~ 0.02 km/s.
- Vrad stability: < 0.5 km/s => decoupled from the central star activities.
- Ve: Ve(C_2, optical) < Ve(CO, radio) by about 1-4 km/s.
- C_2 gas ratational excitation temperature: 410K ~ 800K
- C_2 gas total column density: (2.4 - 8.6) x 10^{14} cm^{-2}
  Ve(C_2) down / Ntotal(C_2) up, Ntotal(C_2) ⇔ dM/dt
- Origin of the circumstellar C_2 gas:
  1) photodissociation of C_2H_2 molecules in the CSE based on the estimated C_2 fractional abundances
  2) photospheric gas outflow considering the great uncertainties in the current model calculations and the observed quantities such as the gas kinetic temperature in the C_2 line-forming region.